

Anisotropic Resistivities of Precisely Oxygen Controlled Single-Crystal $\text{Bi}_2\text{Sr}_2\text{CaCu}_2\text{O}_{8+\delta}$: Systematic Study on “Spin Gap” Effect

T. Watanabe,¹ T. Fujii,² and A. Matsuda^{1,2}

¹*NTT Basic Research Laboratories, 3-1, Morinosato Wakamiya, Atsugi-Shi, Kanagawa 243-01, Japan*

²*Department of Applied Physics, Faculty of Science, Science University of Tokyo, 1-3 Kagurazaka, Shinjuku-ku, Tokyo 162, Japan*
(Received 12 December 1996)

The in-plane resistivity $\rho_a(T)$ and the out-of-plane resistivity $\rho_c(T)$ have been systematically measured for $\text{Bi}_2\text{Sr}_2\text{CaCu}_2\text{O}_{8+\delta}$ single crystals with their oxygen contents precisely controlled. In the underdoped region, deviation from T -linear in-plane resistivity, which evidences the opening of the “spin gap,” is clearly observed, while the out-of-plane resistivity is well reproduced by the activation-type phenomenological formula $\rho_c(T) = (a/T)\exp(\Delta/T) + c$. In contrast to the $\text{YBa}_2\text{Cu}_3\text{O}_{7-\delta}$ system, we find that the onset of the semiconducting $\rho_c(T)$ does not coincide with the opening of the spin gap seen in the $\rho_a(T)$ in this $\text{Bi}_2\text{Sr}_2\text{CaCu}_2\text{O}_{8+\delta}$ system. [S0031-9007(97)04015-5]

PACS numbers: 74.25.Fy, 74.62.Dh, 74.72.Hs

It is well recognized that an understanding of the characteristic electronic phase evolution with carrier doping is important to elucidate the high- T_c superconductivity. One striking phenomena is a “spin gap” state typically observed in underdoped $\text{YBa}_2\text{Cu}_3\text{O}_{7-\delta}$ by various techniques [1] including resistivity measurements [2]. Recently, angle-resolved photoemission spectroscopy (ARPES) [3,4] has directly revealed the normal state pseudogap in an underdoped $\text{Bi}_2\text{Sr}_2\text{CaCu}_2\text{O}_{8+\delta}$ system and pointed out its intimate relation with superconductivity (i.e., $d_{x^2-y^2}$ symmetry). Up to now, however, there have been few transport studies [5,6] of the underdoped state (and thus a spin gap effect) in the $\text{Bi}_2\text{Sr}_2\text{CaCu}_2\text{O}_{8+\delta}$ system. Another striking feature is that a semiconductive out-of-plane resistivity ($d\rho_c/dT < 0$) coexists with metallic in-plane resistivity ρ_a over a wide temperature and carrier doping range [7]. Among the many ideas on the origin of the semiconductive ρ_c , there is a theoretical suggestion [8] that it is caused by the opening of the spin gap in the context of spin charge separation. Experimental results on $\text{YBa}_2\text{Cu}_3\text{O}_{7-\delta}$ [9] seem to be consistent with the theory. However, the mechanism for the out-of-plane conduction is still in dispute [10].

The $\text{Bi}_2\text{Sr}_2\text{CaCu}_2\text{O}_{8+\delta}$ system is a good choice for studying such an electronic phase diagram, because its doping level can be controlled over a wide range by varying the oxygen content. But we encounter several difficulties in controlling the doping level, especially when we go into the underdoped side of the system. One is oxygen inhomogeneity, introduced when a sample is cooled down after an anneal, which causes a broadening of a superconducting phase transition and obscures the intrinsic properties of the system. If samples are rapidly cooled to avoid this problem, high-temperature disorder is frozen. Herein lies the second difficulty. The disorder causes electron localization at low temperatures. The third difficulty is related to the stability of the material. Annealing at high temperatures (≥ 600 °C) and low oxygen pressures ($\leq 10^{-5}$ atm) is needed for realizing the under-

doped state of the $\text{Bi}_2\text{Sr}_2\text{CaCu}_2\text{O}_{8+\delta}$ system. However, these conditions sit close to the decomposing line [11]. We solved all of the above problems by improving the annealing process; the equilibrium oxygen pressures are maintained down to sufficiently low temperature. Details will be shown below.

In this paper, we investigate anisotropic charge transport in $\text{Bi}_2\text{Sr}_2\text{CaCu}_2\text{O}_{8+\delta}$ with carefully controlled oxygen contents, which cover from underdoped ($T_c \approx 70$ K) to slightly overdoped ($T_c \approx 84$ K) states. Clear transport evidence for the existence of the spin gap in the $\text{Bi}_2\text{Sr}_2\text{CaCu}_2\text{O}_{8+\delta}$ system has been obtained in the underdoped in-plane resistivity. The temperature dependence of the out-of-plane resistivity has been analyzed using a phenomenological function. Based on the analysis, we discuss the mechanism for the out-of-plane charge transport, paying special attention to whether the semiconductive ρ_c is relevant to the opening of the spin gap or not.

Single crystals were grown under a mixed gas flow [$\text{O}_2(20\%) + \text{Ar}(80\%)$] using the traveling solvent floating zone method. The validity of the improved annealing process was confirmed by the dc magnetic measurements. The annealed samples showed narrower superconducting transition (≤ 3 K) as well as larger ($\geq 80\%$) Meissner fraction than the as-grown ones (transition width ≈ 5 K, Meissner fraction $\approx 60\%$). The in-plane and the out-of-plane resistivities (ρ_a and ρ_c) were measured in the same manner as in our previous report [12]. The contacts were made from silver epoxy, which ensured low contact resistance (≤ 3 Ω) and did not affect the sample property even after the annealing in very low oxygen pressures.

Figure 1 shows an equilibrium phase diagram on a $\text{Bi}_2\text{Sr}_2\text{CaCu}_2\text{O}_{8+\delta}$ single crystal for various oxygen contents (δ), which was used for the precise control of the carrier doping level. At relatively higher oxygen pressures ($P_{\text{O}_2} \geq 10^{-4}$ atm), the equilibrium lines for each δ were obtained by a thermogravimetric measurement. The absolute value of $\delta = 0.27$ was estimated from the literature on polycrystals [13]. At lower oxygen pressures

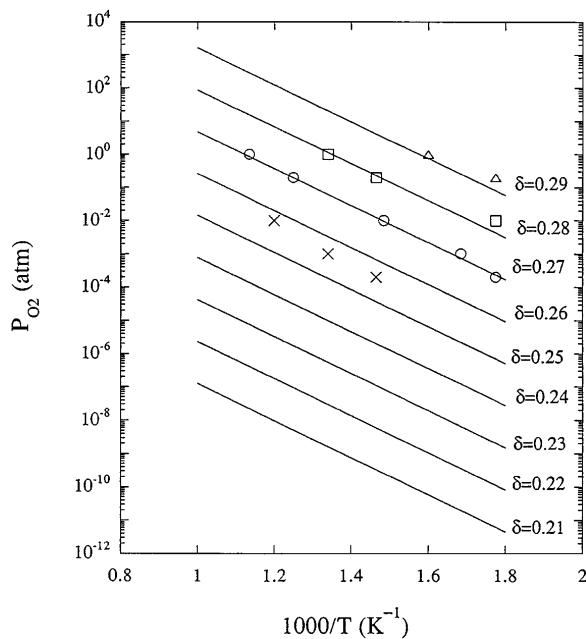


FIG. 1. Equilibrium oxygen partial pressures P_{O_2} versus reciprocal temperature for a $\text{Bi}_2\text{Sr}_2\text{CaCu}_2\text{O}_{8+\delta}$ single crystal for various oxygen contents (δ). Triangles, squares, circles, and crosses are experimentally obtained points for $\delta = 0.29$, $\delta = 0.28$, $\delta = 0.27$, and $\delta = 0.26$, respectively.

($P_{O_2} < 10^{-4}$ atm), the lines are extrapolations from the results obtained at higher oxygen pressures. Thus the absolute values of δ in this phase diagram do not necessarily mean the real oxygen contents; they are only measures of the relative change of the oxygen contents. In order to control δ 's, single crystals were annealed in a quartz tube furnace under the corresponding oxygen partial pressures at 600 °C for 10 h, then slowly cooled (≈ 0.4 °C/min) while keeping the equilibrium oxygen pressures to 300–400 °C. Finally, they were rapidly cooled to room temperature at a rate of about 50 °C/min using an argon flow. For the actual control of the oxygen partial pressures, a mixed gas flow of oxygen and argon at a total amount of 5 l/min was used in the higher oxygen pressure region ($P_{O_2} \geq 10^{-4}$ atm), while in the lower oxygen pressure region ($P_{O_2} < 10^{-4}$ atm); the pressure around the sample was controlled by tuning the conductance of the evacuation path using a slotted valve, as well as by tuning the oxygen flow while continuously evacuating the quartz tube.

Figure 2 shows the temperature dependence of in-plane resistivity ρ_a for $\text{Bi}_2\text{Sr}_2\text{CaCu}_2\text{O}_{8+\delta}$ single crystals with various oxygen contents (δ). The T_c changes systematically with δ . Here again, the quoted values of δ mean that the samples were annealed by a program using those δ of an equilibrium phase diagram shown in Fig. 1. Therefore the accuracy for δ values in actual samples may not be as high as quoted, but we can safely regard δ 's as measures of the relative oxygen contents. The sample with $\delta = 0.27$ shows $T_c = 84$ K. With decreasing δ , T_c increases, indicating the overdoped

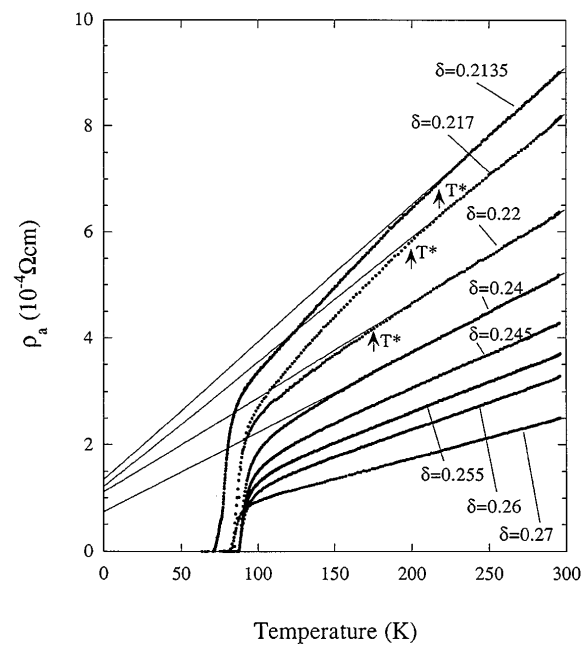


FIG. 2. In-plane resistivities ρ_a of $\text{Bi}_2\text{Sr}_2\text{CaCu}_2\text{O}_{8+\delta}$ single crystals versus temperature for various oxygen contents (δ). The solid straight lines, which are linear extrapolations of ρ_a at higher temperatures, are also shown as a guideline for the near optimally doped ($\delta = 0.24$) and underdoped ($\delta = 0.22$, 0.217, and 0.2135) samples. The temperatures T^* at which the ρ_a deviates from T -linear behavior are shown by arrows for the underdoped samples.

state, and reaches its highest point (optimally doped) of 89–90 K with $\delta = 0.24$ –0.25. Further reduction in δ (≤ 0.22) gives underdoped states with $T_c = 70$ –85 K. The overall slope $d\rho_a/dT$ increases with decreasing δ , indicating that the carrier concentrations (or Drude weight) are actually decreased by the deoxygenation process. A typical T -linear behavior and a slightly upward curvature of ρ_a are also seen in an optimally doped and an overdoped sample, respectively. For the underdoped sample, ρ_a deviates from high-temperature T -linear behavior at a characteristic temperature T^* (shown by the arrow in Fig. 2) far above T_c , and decreases rapidly with decreasing temperature. The T^* was determined as a temperature at which ρ_a decreases 2% from the high temperature T -linear term using a similar analysis shown in Ref. [2]. This behavior is not the effect of superconductive fluctuation; rather, it resembles that observed in underdoped $\text{YBa}_2\text{Cu}_3\text{O}_{7-\delta}$. In this system the behavior has been interpreted as being due to a decrease in spin scattering [2], which is caused by the opening of the spin gap manifested in, for example, the rapid decrease in the NMR relaxation rate T_1^{-1} . T^* increases with decreasing δ ($T^* = 175, 200, 220$ K for $\delta = 0.22, 0.217, 0.2135$, respectively). Further reduction in δ , unfortunately, caused electron localization and obscured such anomalous behavior. T^* can be considered as the temperature at which the pseudogap (observed

recently by ARPES) opens [3,4], since they coincide with each other with respect to their magnitudes as well as their doping-dependent trends. The decrease in the in-plane resistivity ρ_a means that the pseudogap observed in the ARPES experiment is not the type that reduces Fermi surface area, such as charge-density-wave formation, but the type that reduces the scattering rate, such as opening a gap in the spin excitation spectrum. It is natural to consider that the pseudogap in the present and ARPES study is directly related to the spin gap state in a magnetic probe such as NMR, although there is no NMR data available for underdoped $\text{Bi}_2\text{Sr}_2\text{CaCu}_2\text{O}_{8+\delta}$.

Figure 3 shows the temperature dependence of out-of-plane resistivity ρ_c for a $\text{Bi}_2\text{Sr}_2\text{CaCu}_2\text{O}_{8+\delta}$ single crystal (sample I) with various oxygen contents (δ). With decreasing δ , the overall magnitude of ρ_c , as well as its semiconductive temperature dependence, increases. Numerical fits were performed using the functional form proposed by Yan *et al.* [14]; i.e., $\rho_c(T) = (a/T) \exp(\Delta/T) + bT + c$, where a , b , c , and Δ are constants. This fitting was done using the Levenberg-Marquardt algorithm. The fitted curves are shown in Fig. 3 as solid lines, and the parameters obtained are shown as a function of δ in Fig. 4. The fitting results for another sample (sample II) as well as for other studies [14,15] are also shown in Fig. 4. In the overdoped region, the parameter Δ may be overestimated because the ρ_c includes a small component that increasingly diverges at T_c , which can be ascribed to the suppression of the in-plane density of states caused by the superconductive fluctuation effect [16]. In the underdoped

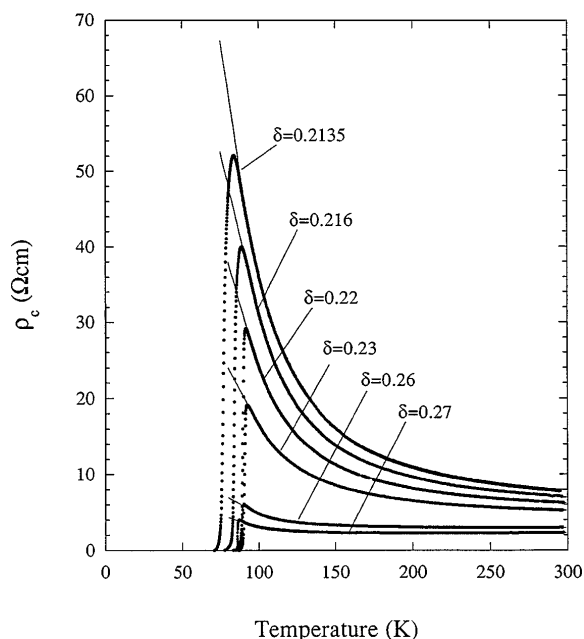


FIG. 3. Out-of-plane resistivities ρ_c of a $\text{Bi}_2\text{Sr}_2\text{CaCu}_2\text{O}_{8+\delta}$ single crystal (sample I) versus temperature for various oxygen contents (δ). The solid curves are numerical fits to $\rho_c(T) = (a/T) \exp(\Delta/T) + bT + c$, where a , b , c , and Δ are constants.

(and also optimally doped) region, the parameter b was set to zero, since the fitting gave it a negative value which was unphysical. We would like to note, however, that the fitting becomes surprisingly better by the setting $b = 0$. The above function of $\rho_c(T)$ has some problem in that it does not cover a whole doping level. Nevertheless, we believe our analysis makes sense, at least for the activation type component. We find that the activation type component is well characterized by the gap Δ for all the doping levels, and the gap Δ is almost constant (≈ 200 K) in the underdoped region. The decrease in parameters a and c with increasing δ would imply an increase in in-plane density of states, if we assume a tunneling mechanism for the out-of-plane conduction.

We have found phenomenologically that the normal state out-of-plane resistivity $\rho_c(T)$ in the optimally doped and underdoped $\text{Bi}_2\text{Sr}_2\text{CaCu}_2\text{O}_{8+\delta}$ is well reproduced by the formula,

$$\rho_c(T) = (a/T) \exp(\Delta/T) + c, \quad (1)$$

(where a , c , and Δ are constants) with almost doping independent Δ (≈ 200 K). The out-of-plane charge

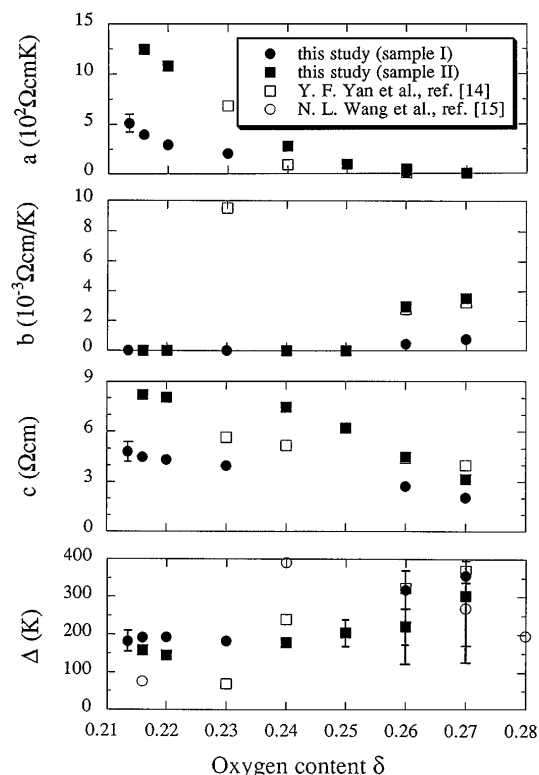


FIG. 4. Parameters obtained by the fits to $\rho_c(T) = (a/T) \exp(\Delta/T) + bT + c$ for various $\text{Bi}_2\text{Sr}_2\text{CaCu}_2\text{O}_{8+\delta}$ single crystals as a function of oxygen contents (δ). Errors for most of the data points are within their marks and are thus not shown. The error bars for Δ on the overdoped samples are drawn largely for the reason mentioned in the text. The δ values for previous reports (Refs. [14] and [15]) were estimated from the reported T_c . Only parameter Δ was available from Ref. [15].

transport is considered as a tunneling process through an insulating barrier because all the values of ρ_c far exceed Mott's limit ($\approx 10^{-2} \Omega \text{ cm}$) [17]. There are several models explaining semiconductive ρ_c ($d\rho_c/dT < 0$) as a finite-temperature effect in a Fermi liquid, for example, interlayer scattering or phonon assisted tunneling [10]. However, recent measurements of the out-of-plane London penetration depth λ_c of high- T_c cuprates show [18] that the strength of the interlayer coupling, which is strongly temperature dependent in the normal state [12], is frozen at T_c . This implies that the origin for the temperature-dependent normal state interlayer coupling lies in its strongly correlated electronic system itself, and the behavior of λ_c is hard to explain with the above models. Moreover, recent measurements by Ando *et al.* [19] on $\text{Bi}_2\text{Sr}_2\text{CuO}_y$ single crystals, in which the semiconductive ρ_c is known to coexist with metallic ρ_a down to the very low temperature (0.66 K) when the superconductivity is destroyed by applying high magnetic field, strongly suggest that the ground state of high- T_c cuprates is non-Fermi-liquid.

Anderson *et al.* [20] have reported that the 2D Luttinger liquid, such as a high- T_c electronic system, always shows "confinement" behavior, which prevents electrons from hopping between layers and realizes semiconductive c -axis transport. Recently, using the t - J model and a slave boson technique, it has been shown [8] that the confinement or the semiconductive behavior can only be realized in the underdoped spin gap state in the phase diagram proposed by Suzumura *et al.* [21]. In this model, an electron is dissociated into a spinon and a holon in the CuO_2 plane, while they must recombine to form an electron in order to tunnel between the planes. When the spin gap opens, the recombination process is suppressed and thus the tunneling rate is reduced. Takenaka *et al.* [9] have shown that the above scenario might be applicable to the $\text{YBa}_2\text{Cu}_3\text{O}_{7-\delta}$ system, because the onset of semiconductive behavior in ρ_c is linked roughly to the onset of nonlinearity in ρ_a . However, we have observed that in the underdoped $\text{Bi}_2\text{Sr}_2\text{CaCu}_2\text{O}_{8+\delta}$ the temperature dependence of ρ_c is always represented by Eq. (1), irrespective of doping level and temperature. That is, semiconductive gap Δ always opens in our measured temperature and doping range, but the spin gap is thought to be open below T^* . The semiconductive ρ_c is also seen in the slightly overdoped sample ($\delta = 0.27$), while no evidence for the spin gap at those doping levels was observed by ARPES [3,4] or in the in-plane resistivity ρ_a . Consequently, we conclude that the semiconductive behavior for ρ_c , at least in $\text{Bi}_2\text{Sr}_2\text{CaCu}_2\text{O}_{8+\delta}$ (and perhaps in high- T_c cuprates), has another origin rather than the spin gap manifested in ρ_a . In this sense, the phase diagram proposed by Suzumura *et al.* [21] (the so-called Fukuyama phase diagram) should be reconsidered.

In summary, based on an intensive study of an anisotropic transport (ρ_a and ρ_c) on the $\text{Bi}_2\text{Sr}_2\text{CaCu}_2\text{O}_{8+\delta}$ system, we have confirmed that the effect of spin gap development manifests in in-plane resistivity ρ_a . Also, we have pointed out that the ρ_c upturn occurs at higher temperature than the so-called spin gap temperature.

We would like to thank Professor R. Yoshizaki for helpful discussions.

Note added.—After the submission of the initial version of this paper, we have observed pseudogap development in the temperature dependence of the vacuum tunneling spectrum for the $\text{Bi}_2\text{Sr}_2\text{CaCu}_2\text{O}_{8+\delta}$ [22]. The pseudogap opening temperature coincides with the onset of semiconductive ρ_c . This suggests that the pseudogap and spin gap effects appear differently on each physical quantity (ρ_c and ρ_a), although it is also possible that they are different phenomena.

-
- [1] J. Rossat-Mignod *et al.*, *Physica* (Amsterdam) **185C-189C**, 86 (1991); J. W. Loram *et al.*, *Phys. Rev. Lett.* **71**, 1740 (1993); C. C. Homes *et al.*, *Phys. Rev. Lett.* **71**, 1645 (1993).
 - [2] T. Ito *et al.*, *Phys. Rev. Lett.* **70**, 3995 (1993).
 - [3] A. G. Loeser *et al.*, *Science* **273**, 325 (1996); D. S. Marshall *et al.*, *Phys. Rev. Lett.* **76**, 4841 (1996).
 - [4] H. Ding *et al.*, *Nature* (London) **382**, 51 (1996).
 - [5] Y. Kotaka *et al.*, *Physica* (Amsterdam) **235C-240C**, 1529 (1994).
 - [6] C. Kendziora *et al.*, *Phys. Rev. B* **45**, 13025 (1992); C. Kendziora *et al.*, *Phys. Rev. B* **48**, 3531 (1993).
 - [7] See, for example, Y. Iye, in *Physical Properties of High Temperature Superconductors III*, edited by D. M. Ginsberg (World Scientific, Singapore, 1992), p. 285.
 - [8] N. Nagaosa, *J. Phys. Chem. Solids* **53**, 1493 (1992); N. Nagaosa *et al.*, *Phys. Rev. B* **45**, 966 (1992); N. Nagaosa, *Phys. Rev. B* **52**, 10561 (1995).
 - [9] K. Takenaka *et al.*, *Phys. Rev. B* **50**, 6534 (1994).
 - [10] S. L. Cooper and K. E. Gray, in *Physical Properties of High Temperature Superconductors IV*, edited by D. M. Ginsberg (World Scientific, Singapore, 1994), p. 61.
 - [11] A. Q. Pham *et al.*, *Physica* (Amsterdam) **194C**, 243 (1992).
 - [12] T. Watanabe and A. Matsuda, *Phys. Rev. B* **54**, R6881 (1996).
 - [13] C. Allgeier *et al.*, *Physica* (Amsterdam) **168C**, 499 (1990).
 - [14] Y. F. Yan *et al.*, *Phys. Rev. B* **52**, R751 (1995).
 - [15] N. L. Wang *et al.*, *J. Low Temp. Phys.* **105**, 951 (1996).
 - [16] L. B. Ioffe *et al.*, *Phys. Rev. B* **47**, 8936 (1993).
 - [17] T. Ito *et al.*, *Nature* (London) **350**, 596 (1991).
 - [18] S. Uchida *et al.*, *Phys. Rev. B* **53**, 14558 (1996).
 - [19] Y. Ando *et al.*, *Phys. Rev. Lett.* **77**, 2065 (1996).
 - [20] P. W. Anderson *et al.*, *Phys. Rev. Lett.* **60**, 132 (1988); P. W. Anderson, *Phys. Rev. Lett.* **67**, 3844 (1991).
 - [21] Y. Suzumura *et al.*, *J. Phys. Soc. Jpn.* **57**, 2768 (1988).
 - [22] A. Matsuda, S. Sugita, and T. Watanabe (unpublished).